Available online at www.sciencedirect.com

SciVerse ScienceDirect

Physics Procedia 37 (2012) 472 – 477

Physics Procedia

TIPP 2011 - Technology and Instrumentation for Particle Physics 2011

Trigger-induced mechanical resonances of gating grid wires in the multi-wire proportional chambers of the ALICE TPC

C.J. Horn[a], A. Junique[b], C. Lippmann[c], M. Mager[b,*], L. Musa[b], T. Richert[d], for the ALICE TPC collaboration

[a]*Vienna UT, Vienna, Austria*
[b]*CERN, Geneva, Switzerland*
[c]*GSI Helmholtzzentrum für Schwerionenforschung mbH, Darmstadt, Germany*
[d]*Lund University, Lund, Sweden*

Abstract

A crucial issue in the design of modern multi-wire proportional chambers (MWPCs) is to avoide mechanical instabilities of thin and long wires that are held at high potentials [1]. Still, these structures are mechanically very sensitive and event-related (random) oscillations have been reported for drift tubes [2, 3], where the gas ionisation originates the driving force.

Gated MWPCs may exhibit a similar effect, recently observed at the ALICE TPC: the trigger-related change of electrostatic potential of the gating grid wires lead to a periodic residual electrostatic force. Albeit rather small (about $10^{-6}\,\mathrm{N\,cm^{-1}}$) it may give rise to sizeable (a few μm) resonant oscillations of the wires. The oscillations result in systematic pick-up signals, with an amplitude comparable to those of minimum ionising particles.

An exhaustive set of measurements, at the detector as well as at a dedicated laboratory set-up with an open chamber, is carried out and forms the subject of this writing.

Keywords: MWPC, gating grid, vibrating string, resonance

1. Introduction

The Time Projection Chamber (TPC) [4] of the ALICE experiment uses multi-wire proportional chambers (MWPCs) to create the electronic signal that is read out in order to record three-dimensional track information. In this paper we report on mechanical resonances induced in the wires used for gating the TPC.

1.1. Motivation

The construction of MWPCs imposes many challenges amongst which is the mechanical stability of the wire planes [5]. Wire chambers of different geometries are known to be sensitive to oscillations, caused by random or event-related forces due to ionisation [2, 3]. These oscillations can lead to a degradation of the detector performance and possibly even break it.

*corresponding author
Email address: Magnus.Mager@cern.ch (M. Mager)

1875-3892 doi:10.1016/j.phpro.2012.02.395

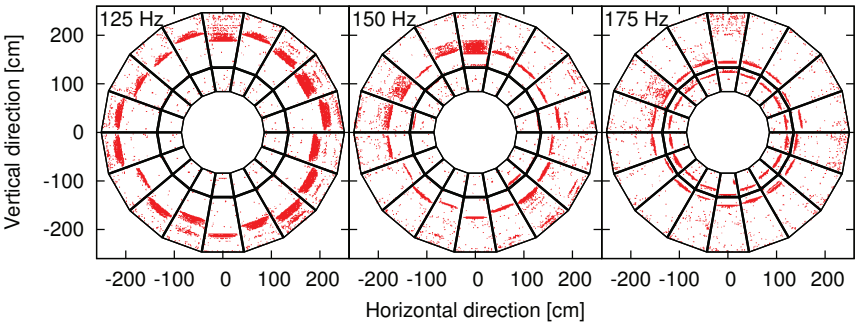

Figure 1. The first observation of the resonances during calibration runs seen as noise in the projection of one side of the TPC for different trigger frequencies.

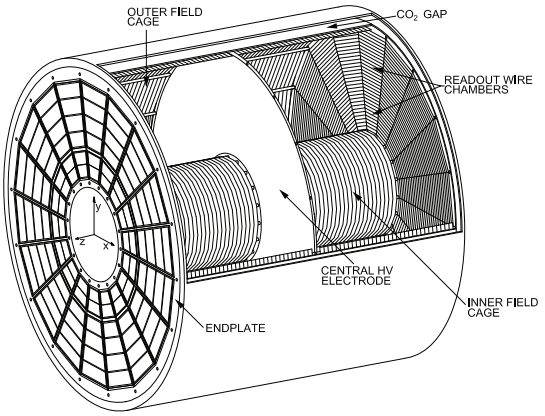

Figure 2. Schematic drawing of the ALICE TPC. (Figure taken from [4].)

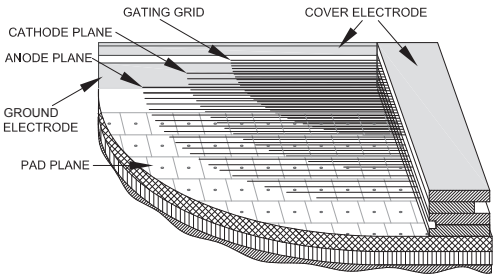

Figure 3. The read-out chambers' wire arrangement. (Figure taken from [4].)

During calibration runs in 2009 a spurious pick-up signal had been noticed at the ALICE TPC. It appears as a line structure at geographical positions on the MWPCs that correlated with the trigger frequency. These structures are shown for three fixed trigger frequencies in Fig. 1. The suspicion—which will be supported in detail in the remainder of this document—was that the chambers act like harps.

1.2. The ALICE TPC

The ALICE TPC is the main tracking device of the ALICE experiment at the Large Hadron Collider (LHC) located at CERN [4]. As shown in Fig. 2 it is made of a hollow cylinder with an active volume of $84.8 < r < 246.6\,\mathrm{cm}$ in radial direction times $|z| < 249.7\,\mathrm{cm}$ in beam direction. It is filled with $90\,\mathrm{m}^3$ of a gas mixture based on Ne (85.7 %), CO_2 (9.5 %), and N_2 (4.8 %) for detection and amplification of the signal[1]. A central high-voltage drift electrode is kept on a potential of $-100\,\mathrm{kV}$ in order to generate a uniform drift field of $400\,\mathrm{V\,cm^{-1}}$ together with the cylindrical field cage and a voltage divider network. Electrons, liberated as a result of gas ionisation by charged particles passing through the TPC, will drift towards one of the two end plates, where the charge is amplified with MWPCs.

The TPC is read out by 72 trapezoidal MWPCs (two sides, each equipped with 18 inner and 18 outer read-out chambers, "IROCs" and "OROCs"), featuring cathode pad read-out with 557 568 sensitive channels. The MWPCs have three wire planes: anode, cathode, and a gating wire grid with lengths range from 27 to 44 cm (IROCs) and 45 to 84 cm (OROCs) as shown in Fig. 3.

[1]The small admixture of N_2 was removed in the year 2011, but had been still present when performing the reported measurements.

Table 1. The properties of the read-out chamber wires [4].

	Anode	Cathode	Gating
Material	Au plated W	Cu/Be (98%/2%)	
Density [g cm^{-3}]	19.25	8.80	
Diameter [µm]	20	75	
Pitch [mm]	2.5	2.5	1.25
	IROC		
Nom. tension [N]	0.45	0.6	
Length [cm]	27 to 44		
Res. frequency [Hz]	310 to 505	200 to 325	
(note)	($E\flat_4$ to B_4)	(G_3 to E_4)	
	OROC		
Nom. tension [N]	0.45	1.2	
Length [cm]	45 to 84		
Res. frequency [Hz]	162 to 303	105 to 195	
(note)	(E_3 to $E\flat_4$)	($A\flat_2$ to G_3)	

Table 2. Differences between laboratory and TPC conditions.

	TPC	Laboratory
Gas	Ne–CO_2–N_2	Air
Composition [vol.%]	85.7–9.5–4.8	—
Density [kg m^{-3}]	1.01	1.28
Kin. viscosity [m^2 s^{-1}]	2.54×10^{-5}	1.45×10^{-5}
Gating Grid potential [V]	70±90	0±90
Drift field [V cm^{-1}]	400	0

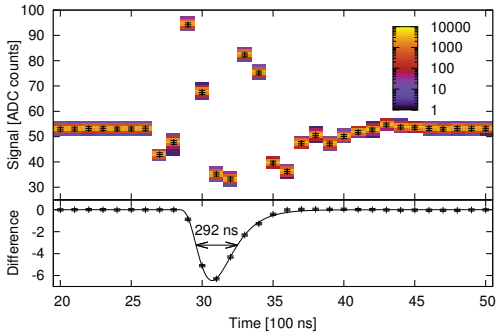

Figure 4. Signal time structure of the induced signal when switching the gating grid (closed→open). The upper part shows the non-resonant case. In resonance the signal deviates from this by the difference shown in the lower part of the plot.

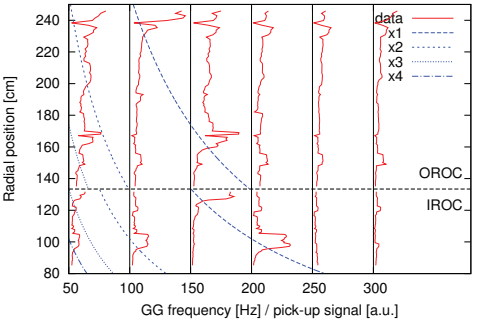

Figure 5. Radial dependence of the induced signal amplitude. Broken lines are fits to the expected dependence and higher harmonics.

The signal is created by electron avalanches around the anode wires inside the high electric field region ("amplification region") that is defined by the cathode plane and the cathode wires. The cathode plane is segmented into pads, and the signal induced on those is read out by the front-end electronics. The gating grid opens when the TPC is triggered, allowing the collection and amplification of the electrons from the drift region. When the gating grid is closed, electrons from the drift region can not enter the amplification region, and positive ions created in the amplification region can not enter the drift region. This prevents the chambers from unnecessary charge collection and highly reduces the build-up of space charge, respectively.

2. Measurements—TPC

When the TPC is triggered, it opens the gating grid and acquires data for a full drift period (100 µs). I. e. all the gating grid wires are held at a potential that makes it transparent for drifting electrons. When the detector is not triggered and electrons are not wanted in the avalanche region, however, the gating grid is closed. The closure of the gating grid is achieved by applying alternating potentials such that every second wire is biased positively/negatively. Even though the signal induced on the pad plane by this biasing should cancel, slight asymmetries lead to a complex but well reproducible signal when the gating grid switches between open and closed mode. It will be induced on top

of the electronics baseline, see Fig. 4. In the resonance case, this signal is super-imposed with a pulse like structure (lower part of Fig. 4), which can be attributed to the spatial asymmetry created by resonant oscillation of the gating grid wires.

The simple model of the vibrating string is adopted to calculate the various properties of resonance in the wire chambers. Thereby, only small excitations of the wires for low frequencies are treated. In this regime the partial differential equations known as the "wave equation", are valid to an excellent extent, yielding the wire resonance frequencies f_0 as:

$$f_0 = \frac{1}{2L}\sqrt{\frac{T}{\varrho_w \pi r^2}}\,. \tag{1}$$

Here L is the wire length, T is the wire stretching force, ϱ_w is the wire density and r is the wire radius, which can be found in Tab. 1 for the different wire planes.

The wires (or strings) are exited when triggering the detector at their characteristic frequencies (and integer parts of them[2]) and lead to a pick-up signal in the data. To carry out a detailed analysis of the induced signal, a thin slice of one TPC sector is read out without post-processing (in particular without zero-suppression) and the data is analysed by comparing data at a given frequency to a reference data set. Figure 4 depicts the signal of a single, representative channel and shows the induced signal for the opening of the gating grid. The lower plot shows how the signal gets distorted under the influence of resonance onto the signal. It has a "pulse-like" structure, comparable in amplitude and time to a minimum ionising particle.

The data is analysed in this way for all recorded channels, and the radial dependence is shown in Fig. 5. The lines in both plots are fits to the expected pick-up signal and resonance frequency dependence, respectively. It is seen that the signal is induced at pads under wires with eigen-frequencies of integer multiples of the gating grid switching frequency. The excitation scales inversely proportional to the frequency ratio as expected from Fourier-analysis.

3. Measurements—Laboratory

In order to verify the characteristics of the resonance phenomenon an IROC is set up in the laboratory for direct optical observation of wire oscillations. Investigations are made to identify the affected wires and their oscillation modes, as well as the temporal dynamics of the oscillation and their amplitude dependence.

3.1. Set-up

A digital microscope, suspended on a side arm, is focussed on the wires of the chamber as shown in Fig. 6. The arm allows for manual displacement and rotation of the microscope. Its extended focal length, accurately adjustable with a micrometer screw, permits to place the microscope at a comfortable distance, a few cm, to the wires.

The pad plane and cathode wires are grounded, while the anode wire voltage can be tuned up to 1350 V and the gating grid voltages are set to 0 V in open mode and alternating ±90 V in closed mode. The microscope has an 1280×1024 pixel CMOS image sensor, which achieves a resolution of about 4 µm. A tilting angle φ, in respect to the chamber plane's normal, leads to a reduction by $\sin(\varphi)^{-1}$ in the maximum resolution. For time-resolved measurement series the set-up is exposed by a stroboscopic light, which enabled steady images at well-known phase correlation to the driving force.

There are slight differences between laboratory set-up and the conditions at the TPC detector (see Tab. 2). First of all there is no central electrode and therefore no electrostatic drift field. The gating grid has no offset voltage of −70 V and, moreover, the measurements are done under normal atmosphere instead of the special gas-mixture. Due to the horizontal position of the chamber, gravity acts in another direction, which leads to a different wire sag. These distinctions lead to a slightly different electrostatic field within the chamber and therefore to different forces acting on the wires. As a result from simulations the net forces are about half times smaller than under real TPC conditions.

[2]This is due to the fact that the time structure of the driving force is rectangular with a small duty cycle and thus has contributions of higher harmonics.

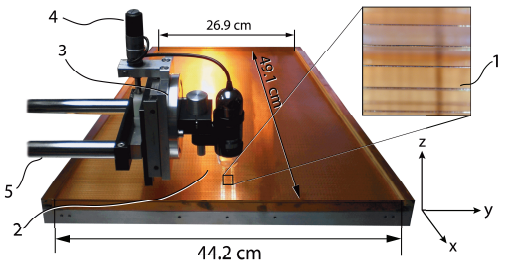

Figure 6. The set-up, featuring: (1) an open IROC with exposed wires; (2) a digital microscope with extended focal length; (3) a rotary suspension with (4) hight adjustment on a (5) movable arm. The whole set-up is exposed by a stroboscopic synchronous light system (not shown).

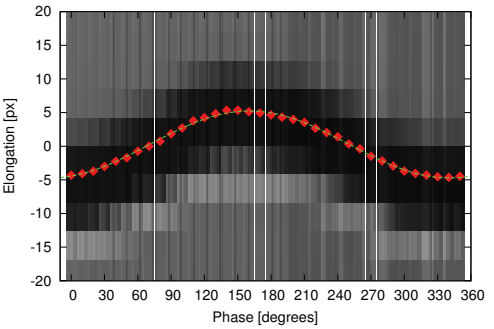

Figure 7. Example of a set of phase shifted acquisitions. The points are the reconstructed center of the wire, the line is a sine fit indicating the precision of the measurement.

3.2. Analysis methods

The measurements are performed in a semi-automatic fashion with an online image recognition system that identifies the wire movements. The employed algorithm consists of the following steps:

1. For each of the 1024 pixel rows the correlation function of the acquired image and a reference image is calculated.
2. The results are quadratically interpolated around their maxima (±1 px) to achieve sub-pixel resolution.
3. The Windsor-mean and -RMS[3] of 1024 results is calculated.

The online analysis software also selects the point in the four-dimensional parameter space (gating-grid opening time and frequency, anode voltage, and phase of the stroboscopic light) to perform the measurement.

To determine the position resolution of the set-up, phase-resolved images of the oscillation is used. It is obtained by shifting the phase of the flash with respect to the driving force. An exemplary result is shown in Fig. 7, indicating the sub-pixel resolution achieved as well as the systematic errors.

3.3. Results

The first basic result from direct observation of the wires is the identification of the oscillating wires and their mode of oscillation: the gating-grid wires oscillate in drift direction (perpendicular to the pad plane). The precise mode of oscillation could be resolved by tilting the viewing angle of the microscope and further observations correspond to a viewing angle of about 45°.

To further analyse the behaviour of the oscillation, a time resolved measurement of the built-up and decay of the resonance was performed. With a refresh rate of the microscope of about six frames per second one can estimate the build up and decay behaviour of the wires only coarsely. Assuming that the experiment is repeatable, however, one may stitch several phase shifted acquisitions together in order to obtain higher frame rates. The outcome of this technique is depicted in Fig. 8, showing that the assumption is valid to a good extent.

In order to see sizable oscillations the gating-grid opening time had to be enlarged to transfer more energy into the system. To extrapolate to the TPC conditions a scan of the dependence of opening time and anode voltage was performed. Theoretically, the amplitude of the oscillations is a linear function of the gating grid opening time (as long as it is short with respect to the oscillation period) and the anode voltage. This is supported by the measurement as shown in Fig. 9. Extrapolated to the TPC conditions (100 µs opening time, 1350 V anode voltage) and taking into account the different gas and electric field configuration we expect a maximum amplitude of 10 µm after a build-up time of about 1 s.

[3] I. e. only the middle-most 50% of the results are taken in order to reduce the influence of outliers or noisy pixels or lines.

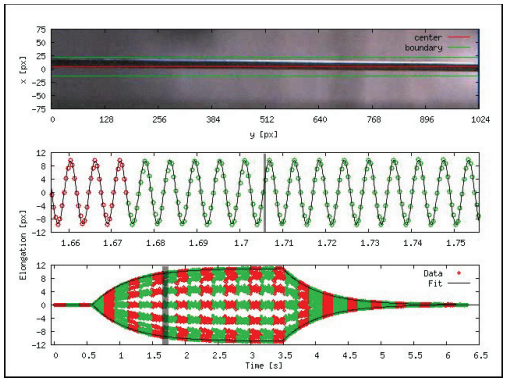

Figure 8. The time resolved buildup and decay of the resonance. Several time shifted acquisitions are overlaid. A single acquisition has alternating red and green points, i. e. a frame rate of about six frames per second. The picture is a single frame of an animation, which may be downloaded from: `http://www-linux.gsi.de/~mmager/TIPP.avi`

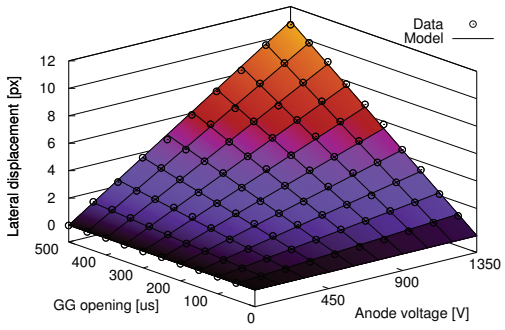

Figure 9. The dependence of the oscillation amplitude on the anode voltage and gating grid opening time. TPC conditions correspond to 1350 V and 100 µs.

4. Summary & Conclusion

Detailed measurements have proved that the net electrostatic forces resulting from the switching of the gating grid electrodes of a TPC may lead to a resonant oscillation of its wires. It is shown how this signal reflects itself in the data and how long it takes to build up. Finally the amplitude dependence is characterized and the maximum amplitude is found to be less than 10 µm—unlikely to cause any damage.

Nevertheless, the resulting pick-up signal has to be taken into account when calibrating the detector and in order to obtain the maximum performance long sequences of equally spaced triggers should be avoided.

Acknowledgments

The authors would like to thank Yannick Lesenechal for the mechanical preparation of the laboratory set-up and Rob Veenhof for his help with simulations.

References

[1] T. Trippe, Minimum tension requirement for Charpak chamber wires, CERN NP Internal Report 69-18 (1969).
[2] I. R. Boyko, G. A. Chelkov, V. I. Dodonov, M. A. Ignatenko, M. Y. Nikolenko, Vibration of signal wires in wire detectors under irradiation, Nucl. Instr. and Meth. A 367 (1 – 3) (1995) 321 – 325.
[3] M. Anderson, J. Godlewski, A. Romaniouk, S. Sutchkov, V. Tikhomirov, Studies of wire vibrations in TRT straw tubes, ATL-INDET-2000-018 (2000).
[4] J. Alme, et al., The ALICE TPC, a large 3-dimensional tracking device with fast readout for ultra-high multiplicity events, Nucl. Instr. and Meth. A 622 (1) (2010) 316 – 367.
[5] J. Dieperink, K. Kleinknecht, P. Steffen, J. Steinberger, T. Trippe, F. Vannucci, Construction problems with large proportional wire chambers, CERN NP Internal Report 69-28 (1969).